metals

MDPI

Article

Enhancing the Mechanical Properties of AZ80 Alloy by Combining Extrusion and Three Pass Calibre Rolling

Shuaiju Meng [1,2], Hui Yu [1,*], Jun Zhou [1], Haisheng Han [1,3,*], Yongyan Li [1], Lishan Dong [1,*], Xiaolong Nan [4], Zhongjie Li [5], Kwang Seon Shin [6] and Weimin Zhao [1,*]

1 School of Materials Science and Engineering, Hebei University of Technology, Tianjin 300130, China; shuaijumeng@163.com (S.M.); zhoujun8610@126.com (J.Z.); liyongyan@126.com (Y.L.)
2 Magnesium Department, Korea Institute of Materials Science, Changwon 51508, Korea
3 Tianjin Key Laboratory of Materials Laminating Fabrication and Interfacial Controlling Technology, Tianjin 300130, China
4 National Key Laboratory of Shock Wave and Detonation Physics, Institute of Fluid Physics, China Academy of Engineering Physics, Mianyang 621999, China; Nanxl@caep.cn
5 School of Materials Science and Engineering, Shannghai Jiao Tong University, Shuanghai 200240, China; lizhongjie1993@126.com
6 Magnesium Technology Innovation Center, School of Materials Science and Engineering, Seoul National University, 1 Gwanak-Ro, Gwanak-Gu, Seoul 08826, Korea; ksshin@snu.ac.kr
* Correspondence: yuhuidavid@126.com (H.Y.); hanhaisheng@hebut.edu.cn (H.H.); donglishan1991@163.com (L.D.); wmzhao@hebut.edu.cn (W.Z.)

Received: 12 January 2020; Accepted: 6 February 2020; Published: 13 February 2020

Abstract: An AZ80 alloy with ultra-high strength and good ductility has been successfully prepared by a novel processing route of combining extrusion and caliber rolling. The caliber rolled (CRed) AZ80 alloy has a necklace grain structure with ultrafine dynamic recrystallized (DRXed) grains formed around the micro-scale deformed grains, which is remarkably different from the uniform microstructure of as-extruded sample free from caliber rolling. In addition, both the deformed region and the DRXed part in CRed AZ80 alloy exhibit more random basal texture than that of the as-extruded sample. Furthermore, the CRed AZ80 alloy demonstrates an excellent comprehensive mechanical property with the ultimate tensile strength of 446MPa and elongation of 13%, respectively. These good mechanical properties of CRed AZ80 alloy can be attributed to the synthetic effects of necklace bimodal microstructure containing ultra-fine grains, profuse $Mg_{17}Al_{12}$ precipitates, and the modified texture.

Keywords: AZ80; caliber rolling; mechanical property; bimodal microstructure

1. Introduction

Owing to the low density and relatively abundant resources of magnesium (Mg), Mg alloys have great potential in lightweight structural applications to meet the increasing lightweight requirement for less pollution emission as well as better fuel efficiency [1,2]. However, their poor mechanical performance inhibits their wider commercial application. A lot of researchers have devoted themselves into developing Mg alloys with good mechanical properties via alloying with rare-earth (RE) elements [3–6], processing by severe plastic deformation (SPD) [7,8] and some other modified processing technologies [9–11]. For example, it was reported that Mg-Gd-Y-Zn-Zr alloy having a tensile yield strength (TYS), an ultimate tensile strength (UTS), and an elongation (EL) of 473 MPa, 542 MPa, and 8.0%, respectively was successfully fabricated [6]. However, this method involving large

amount of RE element will remarkably increases the cost. Some studies have focused on fabricating high-strength RE-free Mg-Al based alloys (TYS > 300 MPa, UTS > 400 MPa UTS) by grain refinement via SPD processing technologies such as equal channel angular pressing (ECAP) [8], accumulative roll bonding (ARB) [12], multi-directional forging (MDF) [13], and high ratio differential speed rolling (HRDSR) [14]. In addition, some newly modified processing technologies such as low temperature slow speed extrusion (LTSS-E) [10] and double extrusion (DE) [11,15], were also explored as choices for producing high performance Mg alloys. However, these processing technologies are inapplicable to commercialize because of limited dimensions, low production efficiency or the complex equipment required [2]. Until now, there is still a great demand for processing technologies that are suitable for manufacturing large-sized high-performance Mg alloys with relatively high efficiency at low cost.

In this respect, caliber rolling was recently introduced as one of the modified rolling processes that can be used for mass production of metal materials with high precision and high strength. Lee et al. [16] fabricated a Ti-Al-V alloy with an ultra-fine grains (<1 μm) by caliber rolling. There is only a small number of researches on caliber rolled (CRed) Mg alloys till now despite its great potential. Mukai et al. [17] found the basal texture weakening effect and the enhancement of TYS when 18 pass caliber rolling was applied to AZ31 alloy. Somekawa et al. [18] revealed that the TYS of as-extruded Mg-Zn alloy was improved to 330 MPa with an EL of 16% after 14 pass caliber rolling. Lee et al. [19] reported that seven pass CRed AZ31 alloy demonstrated TYS, UTS, and EL of 298 MPa, 378 MPa, and 20.9%, respectively. Later, they further [20] fabricated a ZK60 alloy with an ultra-fine-grain structure yielding a UTS of 389 MPa and an EL of 18% by six pass caliber rolling with an area reduction of 84%. All these works demonstrate the great potential of caliber rolling in enhancing the mechanical performance of Mg alloy, but the number of caliber rolling pass applied is too many, leading to the decrease of production efficiency and increase of cost.

In this study, therefore, we present our work in enhancing the mechanical properties of AZ80 by combining extrusion and three pass caliber rolling. In addition, the microstructure was characterized to reveal the strengthen mechanism compared with the as-extruded sample.

2. Materials and Methods

2.1. Materials and Processing

AZ80 Magnesium alloy with composition of Mg-8Al-0.5Zn-0.2Mn (all compositions quoted in present work are in wt. % unless otherwise stated) alloys was prepared using pure Mg, Al, and Zn, as well as Al-5Mn master alloy in an electronic resistance melting furnace. The schematic diagram of sample processing is illustrated in Figure 1. After casting, the billet with a diameter of 60 mm and height of 150 mm was homogenized for 4800 min at 400 °C. Then the billet was extruded at 300 °C at an exit speed of 6 m/min with an extrusion ratio of 25:1. The as-extruded rods with the dimension of Ø12 mm × 50 mm were preheated at 300 °C for 30 min, followed by 3 pass caliber rolling with the diameter of the grooves from 10.6 to 8.7 mm. The accumulated strains of the 3 pass caliber rolling processing is ~40.2%. Then the sample was air-cooled to ambient temperature.

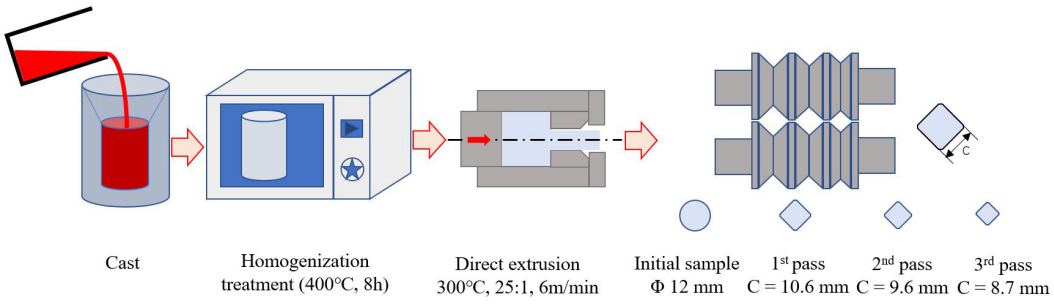

Figure 1. Schematic illustration of cast, homogenization, extrusion and caliber rolling process.

2.2. Characterization

Microstructural characterization of the as-cast, homogenized and as-extruded AZ80 sample was conducted by Olympus (Tokyo, Japan) BX51M optical microscope (OM) and the micro-scale second phases in AZ80 were checked by JEOL (Tokyo, Japan) JSM-7000F scanning electron microscopy (SEM) equipped with energy dispersive spectrometer (EDS). X-ray diffraction (XRD) analysis was conducted using Bruker (Billerica, MA, USA) D8 Focus to figure out the phase in the specimen. For the CRed specimen, OM, SEM, EDS and transmission electron microscope (TEM) installed with energy-dispersive X-ray spectroscopy (EDX) were introduced for the microstructure characterization. Besides, the micro-texture of the CRed sample was characterized by electron back-scatter diffraction (EBSD) compared with as-extruded sample. Metallographic specimens were cut from the as-extruded and CRed AZ80 alloy along the extrusion direction (ED) and rolling direction (RD), respectively. For OM and SEM observation, the samples were mechanically ground and polished, then the prepared samples were etched using a solution made of 4.2 g picric acid, 70 mL ethanol, 10 mL acetic acid and 10 mL distilled water. For TEM analysis, disc samples with a diameter of 3 mm were mechanically polished to a thickness less than 200 μm, and then were ion milled in a Precision Ion Polishing System (GATAN 691). In terms of EBSD specimen, the surface was first ground in the same way as the SEM sample preparation, then polished by colloidal silica for 30 min. HKL Chanel 5 analysis software (OXFORD INSTRUMENTS, Shenyang, China) was used to analysis the EBSD data. The fracture morphologies of both the as-extruded and CRed sample were characterized by SEM after tensile test.

2.3. Mechanical Performance Test

The dog-bone-shaped specimens with the gage dimension of Φ5 mm × 20 mm were adopted for room temperature tensile tests along the ED and RD for the extruded and CRed sample, respectively. The tensile tests were conducted using an electro-universal mechanical testing machine (SUNS-UTM5105X, SHENZHEN SUNS TECHNOLOGY STOCK CO., LTD., Tianjin, China) with an initial strain rate of 1×10^{-3} s^{-1}. All samples were tested at least three times to confirm the repeatability of the mechanical properties.

3. Results and Discussion

3.1. Microstructure of AZ80 Before Calibre Rolling

Figure 2 demonstrates the XRD analysis results of as-cast AZ80 alloy, which is mainly consisted of α-Mg and $Mg_{17}Al_{12}$ phases. Figure 3a,b presents the OM microstructure of the as-cast and homogenized AZ80 alloy, respectively. The as-cast AZ80 microstructure predominantly consists of typically dendritic α-Mg grains and compound networks mostly along the grain boundaries. After homogenization treatment, most of these intermetallic compounds disappear and only a small amount of second particles left in the matrix. The average grain size (AGS) of the homogenized AZ80 sample is ~170 μm. After extrusion, as shown in Figure 3c,d, the AZ80 alloy exhibits a uniform microstructure with an AGS of about 16 μm. Compared with the course microstructure of the homogenized sample, the significantly grain refinement in as-extruded sample indicating the occurrence of fully dynamic recrystallization (DRX) during extrusion.

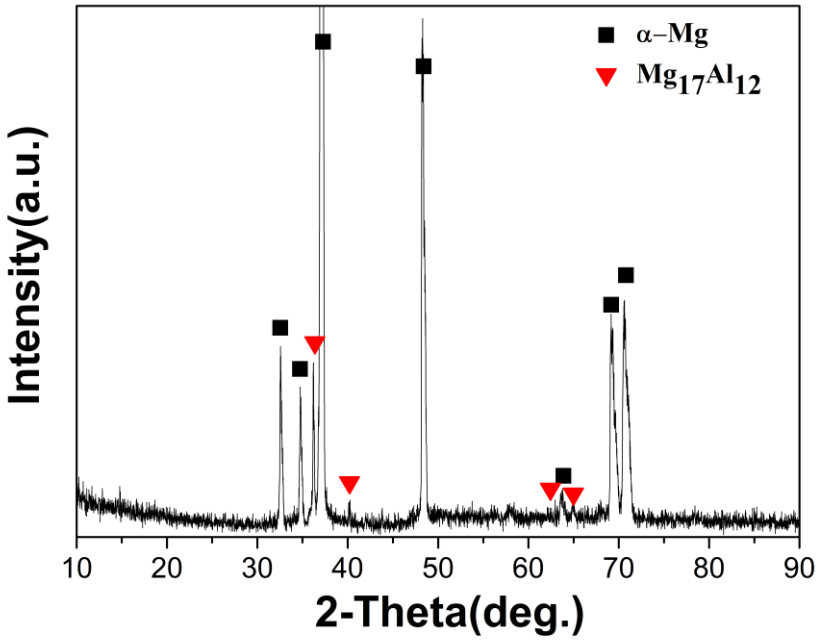

Figure 2. X-ray diffraction (XRD) pattern of the as-cast AZ80 alloy.

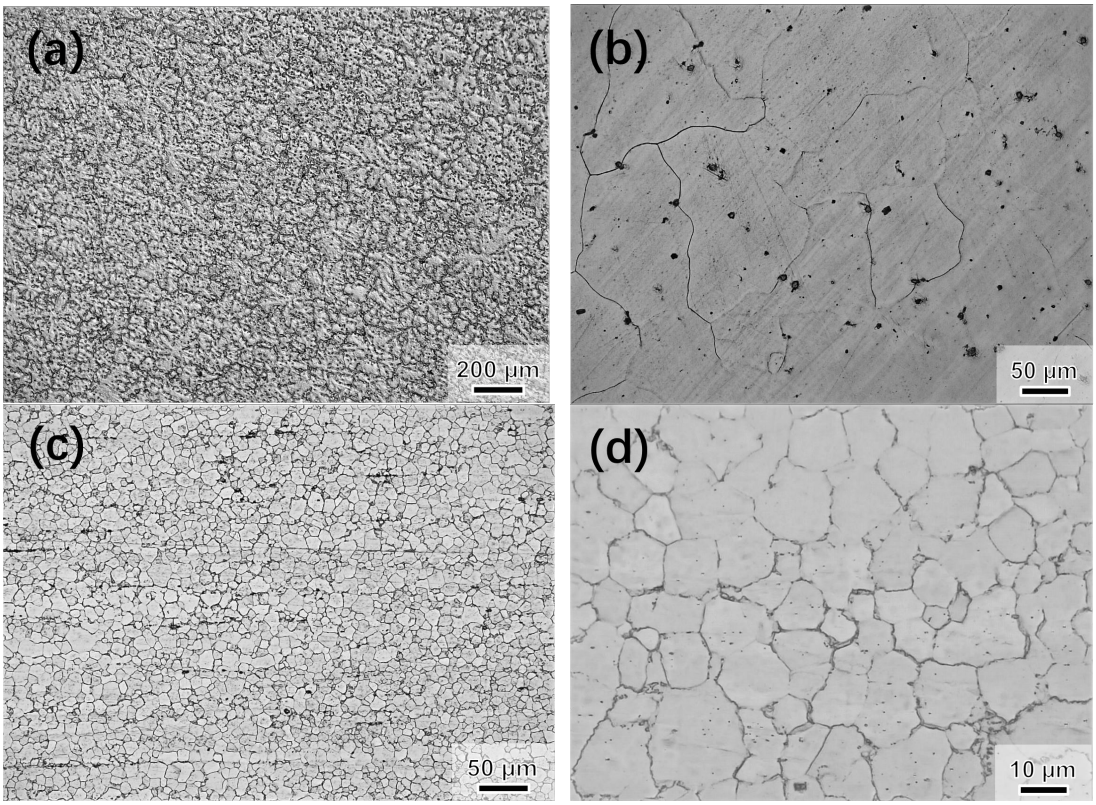

Figure 3. Optical microscope (OM) images of (**a**) the as-cast, (**b**) as-homogenized, and (**c**,**d**) as-extruded AZ80 alloy.

Figure 4 reveals the SEM and EDS analysis result of the as-extruded AZ80 alloy. Both coarse micro-scale compound particles on the matrix and fine precipitates along the grain boundaries and in grain interior were observed. According to the EDS results and our former researches [10,21], the coarse particles containing Al and Mn were Al_8Mn_5 phase particles and those rich of Mg and Al is the undissolved $Mg_{17}Al_{12}$ in AZ80 alloy after homogenization. It should be noted that the Al_8Mn_5

phase in the as-cast AZ80 alloy was not indexed in the above XRD analysis result because of the dilute Mn content (0.2%). The fully DRXed microstructure of the as-extruded AZ80 is most likely because of the relatively high extrusion temperature (300 °C) and high extrusion speed (6 m/min) adopted in this study, which are known to increase the DRX fraction [21]. In addition, the present of micro-scale $Mg_{17}Al_{12}$ and Al_8Mn_5 phase particles with the size of ~10 μm can also contribute to the DRX via generating local inhomogeneity of the strain energy during hot deformation, which is known as particle-simulated nucleation [22,23].

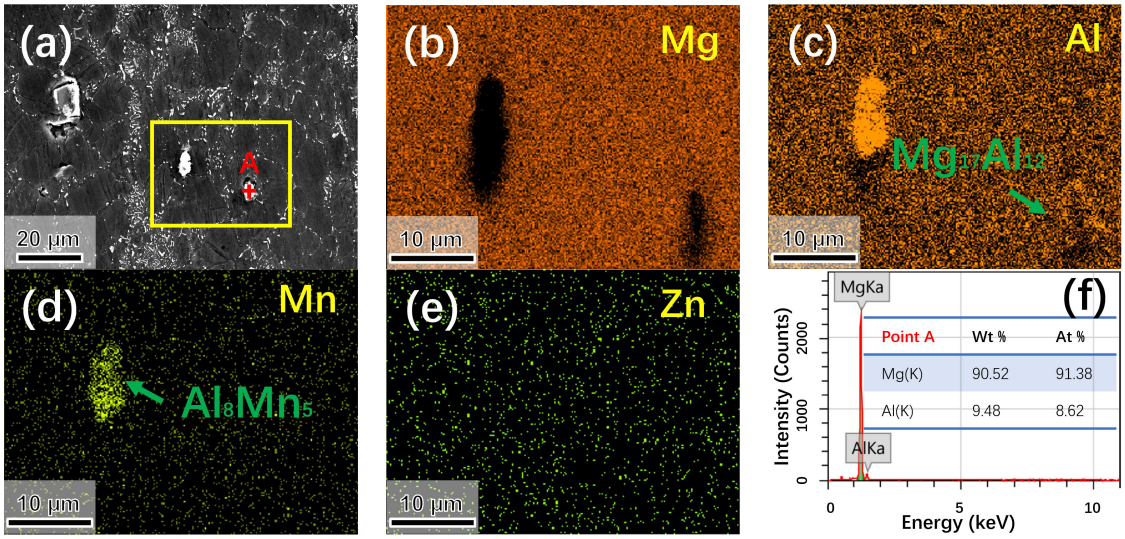

Figure 4. (**a**) Scanning electron microscopy (SEM) microstructure of as-extruded AZ80 alloy; (**b**–**e**) energy dispersive spectrometer (EDS) mapping images of (**b**) Mg, (**c**) Al, (**d**) Mn, and (**e**) Zn, respectively; (**f**) EDS data of the particle A in (**a**) indicating that the marked phase is $Mg_{17}Al_{12}$.

3.2. Microstructure of CRed AZ80

Figure 5 indicates OM, SEM and EDS results of the caliber rolled AZ80 alloy. Different from the homogeneous microstructure of the as-extruded sample, the CRed sample exhibits a typical bimodal microstructure consisting of deformed grains original from as-extruded state and much finer grains formed around the deformed grains. This necklace bimodal microstructure of CRed AZ80 alloy indicates that DRX occurred during the 3 pass caliber rolling at 300 °C, which is commonly observed during multiple pass caliber rolling of AZ31 [24]. The second phases are more clearly observed in the SEM images, as shown in Figure 5c,d, both micro-scale and nano-scale second phase particles were detected. Furthermore, EDS results (Figure 5e,f) confirm that the micro-scale second phases include both Mg-Al and Al-Mn phases, which can be identified as $Mg_{17}Al_{12}$ and Al_8Mn_5, respectively. The Mg element was also detected in particle B, which is from the matrix where the Al_8Mn_5 phase particles distributed on.

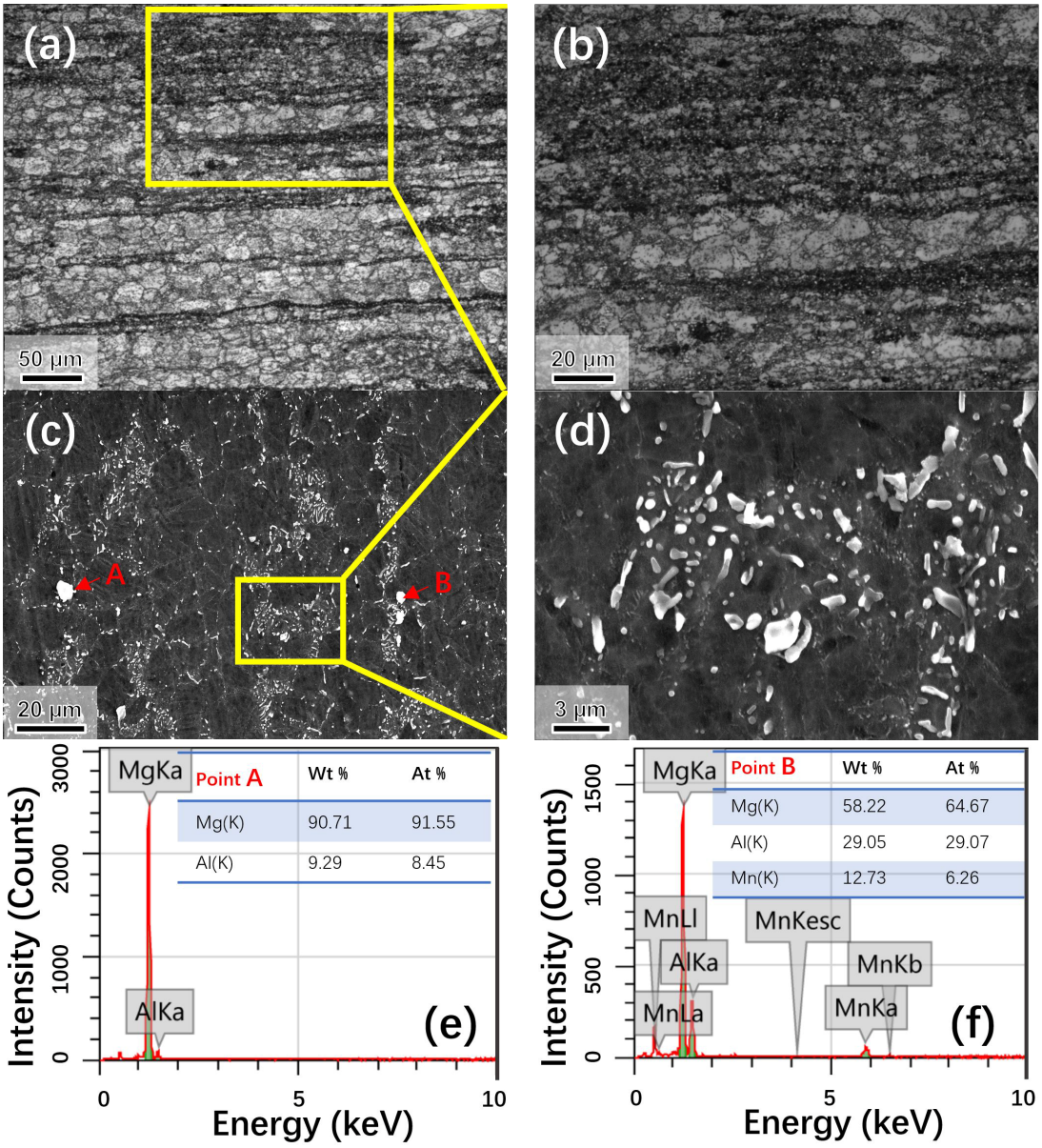

Figure 5. (**a**,**b**) Ooptical microscope (OM) and (**c**,**d**) SEM micrographs of CRed AZ80 alloy; (**e**,**f**) EDS data of (**e**) particle A and (**f**) particle B in (**c**).

In order to further characterize the bimodal structure and micro-texture of CRed AZ80 alloy, an EBSD experiment was conducted on both as-extruded and CRed AZ80 alloy, as demonstrated in Figure 6. The as-extruded AZ80 alloy exhibits a homogeneous microstructure with an AGS of ~15 μm, which is well agreed with OM observation results (Figure 3c,d). After three pass caliber rolling, both the deformed coarse grains and ultra-fine DRXed grains with diameter ~1 μm with the volume fraction of ~25% can be observed clearly along the boundaries of the deformed grains in the inverse pole figure (IPF) maps (Figure 6b–d). Besides, the necklace bimodal characteristics of the sample after three pass caliber rolling indicates the occurrence of discontinuous DRX (DDRX) during rolling process at 300 °C. In addition, both the as-extruded and the CRed AZ80 alloy exhibit basal fiber texture (Figure 6e,f) with the {0001} plane and the <01$\bar{1}$0> direction of the grains in as-extruded and CRed samples mainly oriented parallel to the ED and RD, respectively. However, the maximum texture intensity of the AZ80 alloy decreases from 4.17 multiples uniform density (mud.) to 2.65 mud after three pass caliber rolling, indicating that the texture weakening benefit of caliber rolling. It should be noted that more randomized texture is generated with the ultra-fine DRXed grains than that of the

deformed grains in the CRed sample, as indicated in Figure 6g,h. The result is consistent with previous research on the texture components transition during DRX [23]. And the basal texture weakening effect of caliber rolling processing on extruded Mg alloy is also revealed in the research on AZ31 by Mukai et al. [17], which is mainly caused by the shear deformation. As a result, a bulk Mg alloy having necklace-like structure and modified basal texture was successfully fabricated by combining two simple thermomechanical processing in present study.

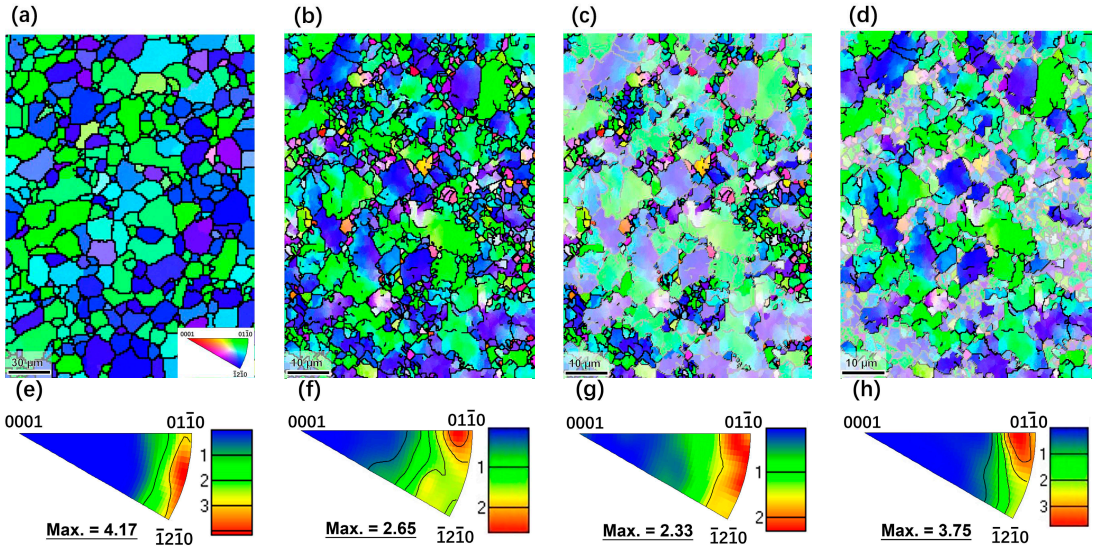

Figure 6. (**a**–**d**) Inverse pole figure (IPF) maps and (**e**–**h**) IPFs of (**a**,**e**) as-extruded and (**b**–**d**,**f**–**h**) CRed AZ80 alloy, respectively; (**b**,**f**) overall; (**c**,**g**) DRXed; (**d**,**h**) unDRXed regions of CRed AZ80 alloy.

A TEM experiment were also carried out to further reveal the bimodal microstructure and the precipitation behavior of the CRed sample. Bright field TEM images of the CRed AZ80 alloy are displayed in Figure 7. As exhibited in Figure 7a,b, lots of sub-grains can be detected in the deformed matrix, indicated by the green arrows. It is thus hypothetical that these sub-grain boundaries can also play a role in generating the potential nuclei of recrystallization. Besides, as indicated by the red arrows in Figure 7b, nano precipitates are found to be distributed near these sub-grain boundaries. In addition, the typical TEM image of the ultra-fine microstructure in CRed AZ80 is presented in Figure 7c,d. The DRXed grains that formed during caliber rolling have the grain size of ~0.85 μm. Nano precipitates were also detected in the matrix of ultra-fine grains area (Figure 7d). Based on the indexed result of the selected area electron diffraction pattern, these nano-scale precipitation particles are confirmed as $Mg_{17}Al_{12}$ (bcc, a = b = c = 1.056 nm). These spherical $Mg_{17}Al_{12}$ particles are mainly formed during extrusion as a result of dynamic precipitation [23]. During caliber rolling at 300 °C, these pre-existing phases are believed to restrict the grain growth of the DRXed grains after nucleation by pinning effect, which will contribute to the formation of ultra-fine DRXed grain structure [25–27]. Surprisingly, the ultra-fine grain size of AZ80 alloy (~0.85 μm), which is effectively pined by nano-precipitates during caliber rolling, is even finer than that of 18 pass caliber rolled AZ31 (1.5 μm) [17]. Furthermore, the ultra-fine grain structure is even comparable with that obtained by double extruded Mg-Ca alloy (~0.7 μm) [11], and the ultra-high strength Mg-2Sn-2Ca (TX22) alloy (~0.65 μm) extruded at low temperature (200–240 °C) [28]. Accordingly, the submicron grain size, nano precipitates in present CRed AZ80 alloy can necessarily contribute to good mechanical performance. Based on the above EBSD and TEM results, it can be concluded that the bimodal microstructure of CRed AZ80 sample can be mainly owing to the DDRX that mainly occurred along the grain boundaries of the as-extruded sample during rolling process. Furthermore, the abundant precipitation of nano $Mg_{17}Al_{12}$ particles greatly contributes to the formation of the ultra-fine grains in the necklace structure by pinning effect.

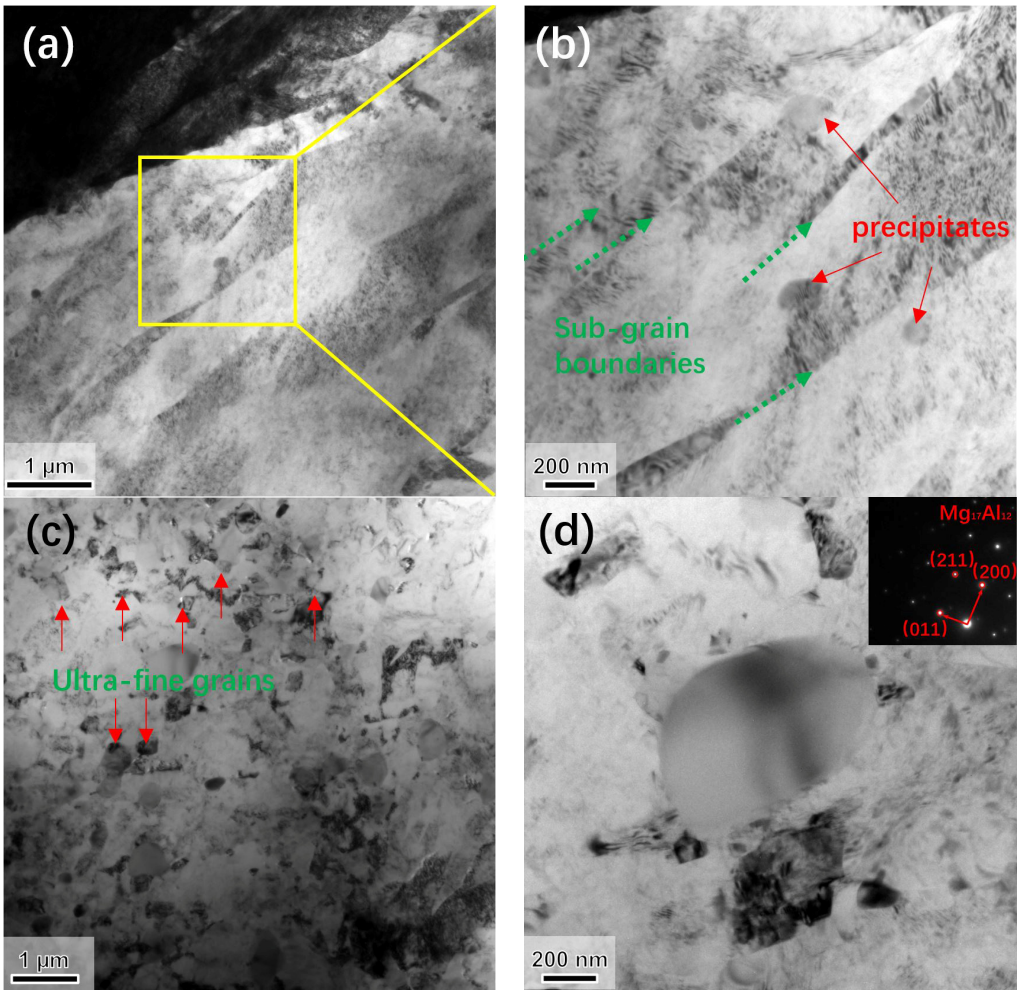

Figure 7. Transmission electron microscope (TEM) images of (**a**,**b**) unDRXed and (**c**) DRXed microstructure of CRed AZ80 alloy; (**d**) image of precipitate in CRed AZ80 alloy (inset in (**d**): $Mg_{17}Al_{12}$ diffraction pattern).

3.3. Mechanical Properties

The representative tensile stress-strain curves of the CRed AZ80 sample is shown in Figure 8 compared with that of the as-extruded sample and their related tensile properties are listed in Table 1. As-extruded AZ80 alloy demonstrates the TYS, UTS, and EL of 227 MPa, 327 MPa, and 20%, respectively. After three pass caliber rolling, the strength of the CRed AZ80 alloy was greatly enhanced with TYS and UTS being 370 MPa and 446 MPa, respectively, both much higher than those of the corresponding as-extruded sample. The comparison of CRed AZ80 in this study with the other recently developed high strength Mg alloys [4,6,8–14,17,19,21,28–31] is shown in Figure 9. The UTS of the CRed AZ80 sample are much higher than those previously reported high strength Mg-8Al-4Sn-2Zn [21], Mg-10Sn-1Al-1Zn [29], Mg-3.5Al-3.3Ca-0.4Mn [30], and Mg-2Sn-2Ca [28] alloys. Besides, The ultra-high UTS of the CRed AZ80 fabricated here is even higher than that of LTSS-extruded AZ80 [10], 18 pass CRed AZ31 [17], HPRed AZ91 [9], HRDSRed AZ91 [12], ARBed AZ91 [13], 20 pass MDFed AZ61 [14], as well as the ECAPed Mg-8Gd-3Y-1Zn containing long-period stacking ordered phases [31].

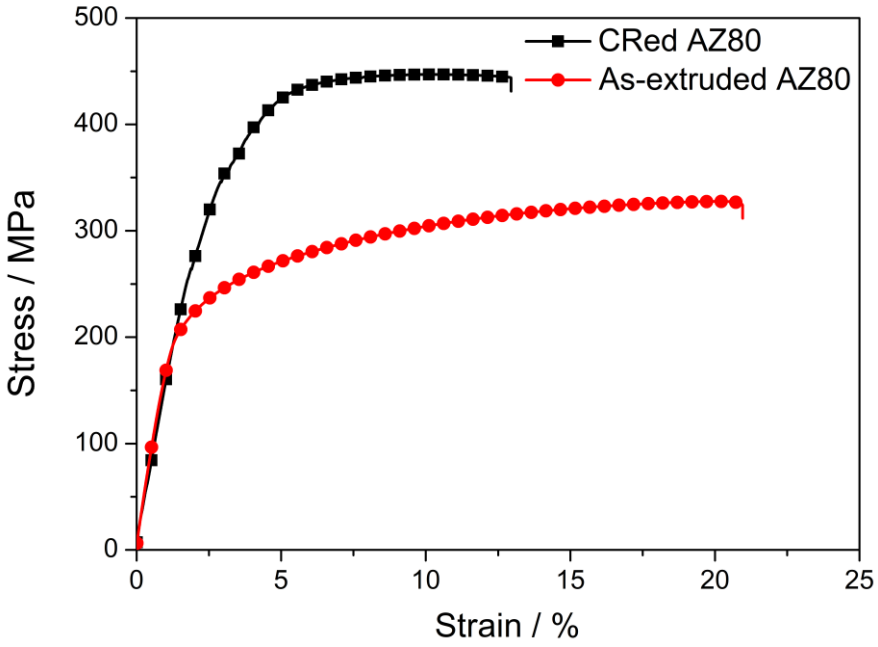

Figure 8. Typical tensile stress-strain curves of CRed AZ80 alloy compared with as-extruded AZ80 sample.

Table 1. Tensile properties of CRed AZ80 compared with as-extruded sample.

Alloys	Process Parameters	TYS (MPa)	UTS (MPa)	EL (%)
AZ80	E [1] + 3 pass CR [2], 300 °C	370 ± 3	446 ± 5	13 ± 1
AZ80	E, 300 °C, 6 m/min	227 ± 4	327 ± 3	20 ± 2

[1] E: extrusion; [2] CR: caliber rolling.

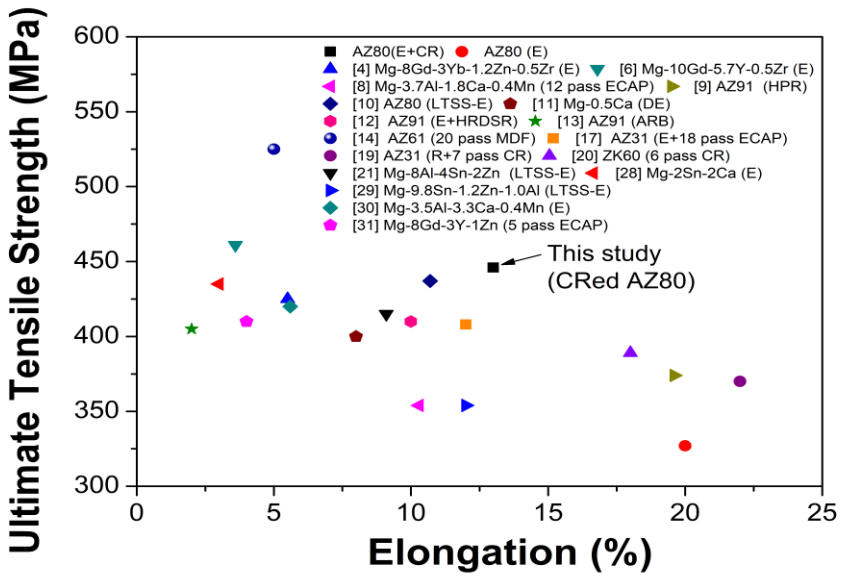

Figure 9. Comparison of UTS vs. EL of CRed AZ80 with previously reported wrought Mg Alloys [4,6,8–14,17,19,21,28–31] (E: Extrusion; CR: Calibre rolling; ECAP: Equal channel angular pressing; HPR: Hard plate rolling; LTSS-E: low temperature slow speed extrusion; DE: Double extrusion; HRDSR: High-ratio differential speed rolling; ARB: Accumulative roll bonding; R: Rolling; MDF: Multi-directional forging).

On the other hand, the CRed AZ80 sample demonstrates a lower EL (13%) than that of the as-extruded sample (20%). This can be explained by the evidence observed on the fracture surface after tensile test, as shown in Figure 10. Both the as-extruded and CRed AZ80 samples demonstrate ductile characteristic with plenty of dimples on the surface. In addition, micro-scale second phase particles can be observed in fracture surface of the two sample (Figure 10a,c), which is constant with the above microstructure characterization results. However, the surface morphology of the as-extruded sample is more uniform than that of the CRed one, owing to the homogenized and bimodal microstructure of as-extruded and CRed samples, respectively. Besides, the dimples in the CRed sample there are much smaller and shallower than those of the as-extruded sample, as compared in Figure 10b,d. As the strain hardening ability of ultra-fine grain area is lower than that of the micro-scale grain area [23], the inhomogeneous deformation between ultra-fine grains and microscale deformed grains in CRed sample will cause the initiation of fracture, thus decrease the ductility of the CRed AZ80 alloy.

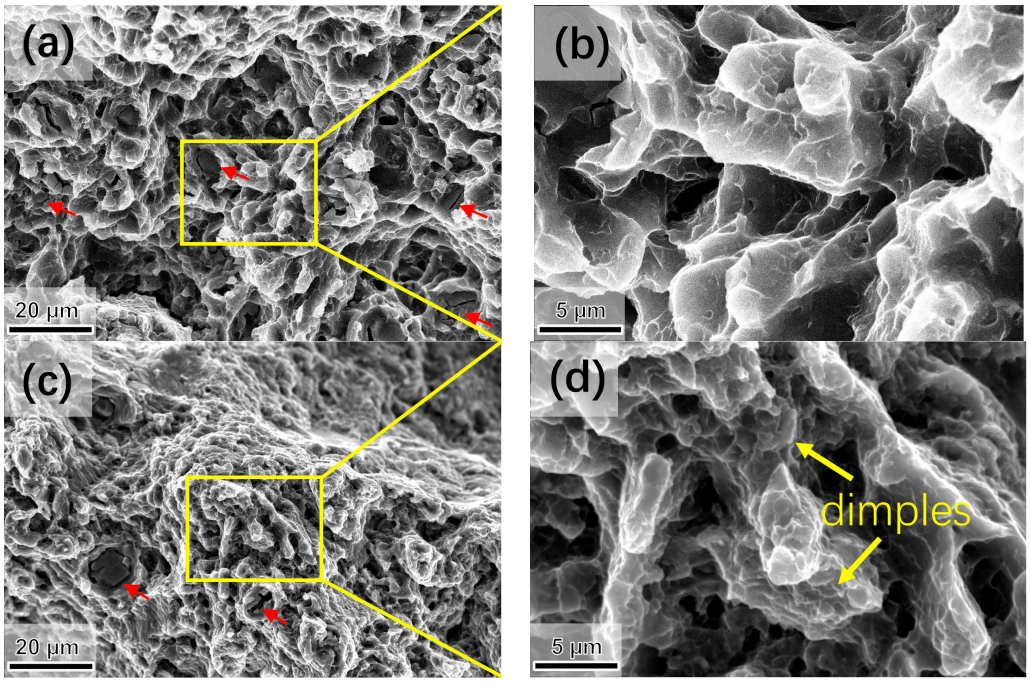

Figure 10. SEM fracture morphology of (**a**,**b**) as-extruded and (**c**,**d**) CRed AZ80 alloy after tensile test to failure.

Furthermore, the CRed AZ80 alloy still demonstrates a good ductility with the EL of 13%. Though the EL of CRed AZ80 is lower than that of as-extruded AZ80 sample (20%), the ductility of the CRed AZ80 fabricated here is much higher compared with those of other ultra-high strength Mg alloys [4,6,8,10,12–14,19,21,28–31].

Based on the above microstructure characterization results, the good comprehensive mechanical performance of the CRed AZ80 alloy can be mainly attribute to the necklace bimodal structure containing ultra-fine grains. A good combination of both high strength and high ductility was also observed in a necklace bimodal structured Mg-9Al-1Zn alloy fabricated by hard plate rolling (HPR) recently [9]. It has been proposed as a good way to produce metal materials having both high strength and good ductility by introducing a bimodal microstructure [32,33]. It was reported that the ultra-fine grains provide the high strength, while the coarser grains enable strain hardening by providing more space to accommodate dislocations in the bimodal microstructure alloys containing ultra-fine grains [10,34]. Besides, the ultra-high strength of the CRed AZ80 will be further contributed by precipitation strengthening from fine $Mg_{17}Al_{12}$ precipitates, solid-solution strengthening from dissolved Al and Zn, as well as the dispersion strengthening from relatively large Al_8Mn_5 and $Mg_{17}Al_{12}$ phases. On the other hand, the necklace bimodal microstructure with more random basal texture

will also benefit the dislocation glide on basal planes, which enhanced the ductility of CRed AZ80 alloy [35,36].

4. Conclusions

In summary, a commercially available RE-free AZ80 alloy with excellent comprehensive mechanical property was successfully produced by a novel processing route of combining extrusion and three pass caliber rolling. The CRed AZ80 sample exhibits an ultra-high strength with UTS of ~446 MPa and at the same time a good ductility with EL of ~13%, respectively. The attractive mechanical performance is mainly originated from the combined effects of necklace bimodal microstructure containing ultra-fine grains, profuse $Mg_{17}Al_{12}$ precipitates, and the modified texture. Overall, the simple combination of two commercially adopted extrusion and caliber rolling processing is expected to inspire a new processing method for fabricating high performance Mg based materials products for large-scale industrial applications.

Author Contributions: Methodology, S.M., H.Y., and H.H.; data curation, S.M., H.Y., J.Z., and L.D.; formal analysis, J.Z. and Y.L.; investigation, S.M., H.Y., H.H., L.D., X.N., and Z.L.; resources, H.H., X.N., Z.L., K.S.S., and W.Z.; writing—Original draft preparation, S.M., H.Y.; writing—Review and editing, S.M., H.Y., J.Z., H.H., Y.L., L.D., X.N., Z.L., K.S.S., and W.Z.; supervision, H.Y., H.H., L.D., and W.Z.; project administration, W.Z. and H.Y. All authors have read and agreed to the published version of the manuscript.

Funding: The authors acknowledge financial support from the National Natural Science Foundation of China (51701060, 51601181), the Natural Science Foundation of Tianjin city (18JCQNJC03900), The Scientific Research Foundation for the Returned Overseas Chinese Scholars of Hebei Province (C20190505), 100 Foreign Experts Plan of Hebei Province (141100), Foundation strengthening program (2019-JCJQ-142), National Research Council of Science and Technology (NST) grant by the Korea government (MSIP) (CRC-15-06-KIGAM) and the Joint Doctoral Training Foundation of HEBUT (2018HW0008).

Conflicts of Interest: The authors declare no conflict of interest.

References

1. Suh, B.C.; Shim, M.S.; Shin, K.S.; Kim, N.J. Current issues in magnesium sheet alloys: Where do we go from here? *Scr. Mater.* **2014**, *84*, 1–6. [CrossRef]
2. Meng, S.J.; Yu, H.; Fan, S.D.; Li, Q.Z.; Park, S.H.; Suh, J.S.; Kim, Y.M.; Nan, X.L.; Bian, M.Z.; Yin, F.X.; et al. Recent Progress and Development in Extrusion of Rare Earth Free Mg Alloys. *Acta Metall. Sin. (Engl. Lett.)* **2019**, *32*, 145–168. [CrossRef]
3. Tekumalla, S.; Seetharaman, S.; Almajid, A.; Gupta, M. Mechanical Properties of Magnesium-Rare Earth Alloy Systems: A Review. *Metals* **2015**, *5*, 1–39. [CrossRef]
4. Li, B.; Guan, K.; Yang, Q.; Niu, X.; Zhang, D.; Lv, S.; Meng, F.; Huang, Y.; Hort, N.; Meng, J. Microstructures and mechanical properties of a hot-extruded Mg-8Gd-3Yb-1.2Zn-0.5Zr (wt%) alloy. *J. Alloys Compd.* **2019**, *776*, 666–678. [CrossRef]
5. Wu, G.; Jafari Nodooshan, H.R.; Zeng, X.; Liu, W.; Li, D.; Ding, W. Microstructure and High Temperature Tensile Properties of Mg–10Gd–5Y–0.5Zr Alloy after Thermo-Mechanical Processing. *Metals* **2018**, *8*, 980. [CrossRef]
6. Homma, T.; Kunito, N.; Kamado, S. Fabrication of extraordinary high-strength magnesium alloy by hot extrusion. *Scr. Mater.* **2009**, *61*, 644–647. [CrossRef]
7. Vinogradov, A.; Vasilev, E.; Kopylov, V.I.; Linderov, M.; Brilevesky, A.; Merson, D. High Performance Fine-Grained Biodegradable Mg-Zn-Ca Alloys Processed by Severe Plastic Deformation. *Metals* **2019**, *9*, 186. [CrossRef]
8. Wang, C.; Ma, A.; Sun, J.; Zhuo, X.; Huang, H.; Liu, H.; Yang, Z.; Jiang, J. Improving Strength and Ductility of a Mg-3.7Al-1.8Ca-0.4Mn Alloy with Refined and Dispersed Al2Ca Particles by Industrial-Scale ECAP Processing. *Metals* **2019**, *9*, 767.
9. Zha, M.; Zhang, X.H.; Zhang, H.; Yao, J.; Wang, C.; Wang, H.Y.; Feng, T.T.; Jiang, Q.C. Achieving bimodal microstructure and enhanced tensile properties of Mg-9Al-1Zn alloy by tailoring deformation temperature during hard plate rolling (HPR). *J. Alloys Compd.* **2018**, *765*, 1228–1236. [CrossRef]

10. Yu, H.; Park, S.H.; You, B.S. Development of extraordinary high-strength Mg-8Al-0.5Zn alloy via a low temperature and slow speed extrusion. *Mater. Sci. Eng. A* **2014**, *610*, 445–449. [CrossRef]
11. Ikeo, N.; Nishioka, M.; Mukai, T. Fabrication of biodegradable materials with high strength by grain refinement of Mg-0.3 at% Ca alloys. *Mater. Lett.* **2018**, *223*, 65–68. [CrossRef]
12. Pérez-Prado, M.T.; del Valle, J.A.; Ruano, O.A. Achieving high strength in commercial Mg cast alloys through large strain rolling. *Mater. Lett.* **2005**, *59*, 3299–3303. [CrossRef]
13. Miura, H.; Maruoka, T.; Yang, X.; Jonas, J.J. Microstructure and mechanical properties of multi-directionally forged Mg-Al-Zn alloy. *Scr. Mater.* **2012**, *66*, 49–51. [CrossRef]
14. Kim, W.J.; Jeong, H.G.; Jeong, H.T. Achieving high strength and high ductility in magnesium alloys using severe plastic deformation combined with low-temperature aging. *Scr. Mater.* **2009**, *61*, 1040–1043. [CrossRef]
15. Huang, H.; Miao, H.; Yuan, G.; Wang, Z.; Ding, W. Fabrication of ultra-high strength magnesium alloys over 540 MPa with low alloying concentration by double continuously extrusion. *J. Magnes. Alloy.* **2018**, *6*, 107–113. [CrossRef]
16. Lee, T.; Shih, D.S.; Lee, Y.; Lee, C.S. Manufacturing Ultrafine-Grained Ti-6Al-4V Bulk Rod Using Multi-Pass Calibre-Rolling. *Metals* **2015**, *5*, 777–789. [CrossRef]
17. Mukai, T.; Somekawa, H.; Inoue, T.; Singh, A. Strengthening Mg-Al-Zn alloy by repetitive oblique shear strain with calibre roll. *Scr. Mater.* **2010**, *62*, 113–116. [CrossRef]
18. Somekawa, H.; Singh, A.; Inoue, T. Enhancement of toughness by grain boundary control in magnesium binary alloys. *Mater. Sci. Eng. A* **2014**, *612*, 172–178. [CrossRef]
19. Lee, J.H.; Kwak, B.J.; Kong, T.; Park, S.H.; Lee, T. Improved tensile properties of AZ31 Mg alloy subjected to various calibre-rolling strains. *J. Magnes. Alloy.* **2019**, *7*, 381–387. [CrossRef]
20. Lee, T.; Kwak, B.J.; Kong, T.; Lee, J.H.; Lee, S.W.; Park, S.H. Enhanced yield symmetry and strength-ductility balance of calibre-rolled Mg-6Zn-0.5Zr with ultrafine-grained structure and bulk dimension. *J. Alloys Compd.* **2019**, *803*, 434–441. [CrossRef]
21. Park, S.H.; Jung, J.-G.; Kim, Y.M.; You, B.S. A new high-strength extruded Mg-8Al-4Sn-2Zn alloy. *Mater. Lett.* **2015**, *139*, 35–38. [CrossRef]
22. Meng, S.; Yu, H.; Zhang, H.; Cui, H.; Wang, Z.; Zhao, W. Microstructure and mechanical properties of extruded pure Mg with Bi addition. *Acta Metall. Sin.* **2016**, *52*, 811–820.
23. Meng, S.; Yu, H.; Zhang, H.; Cui, H.; Park, S.H.; Zhao, W.; You, B.S. Microstructure and mechanical properties of an extruded Mg-8Bi-1Al-1Zn (wt%) alloy. *Mater. Sci. Eng. A* **2017**, *690*, 80–87. [CrossRef]
24. Inoue, T.; Somekawa, H.; Mukai, T. Hardness Variation and Strain Distribution in Magnesium Alloy AZ31 Processed by Multi-pass Calibre Rolling. *Adv. Eng. Mater.* **2009**, *11*, 654–658. [CrossRef]
25. Jung, J.-G.; Park, S.H.; Yu, H.; Kim, Y.M.; Lee, Y.-K.; You, B.S. Improved mechanical properties of Mg–7.6Al–0.4Zn alloy through aging prior to extrusion. *Scr. Mater.* **2014**, *93*, 8–11. [CrossRef]
26. Robson, J.D.; Henry, D.T.; Davis, B. Particle effects on recrystallization in magnesium-manganese alloys: Particle pinning. *Mater. Sci. Eng. A* **2011**, *528*, 4239–4247. [CrossRef]
27. Jung, J.-G.; Park, S.H.; You, B.S. Effect of aging prior to extrusion on the microstructure and mechanical properties of Mg-7Sn-1Al-1Zn alloy. *J. Alloys Compd.* **2015**, *627*, 324–332. [CrossRef]
28. Pan, H.; Qin, G.; Huang, Y.; Ren, Y.; Sha, X.; Han, X.; Liu, Z.-Q.; Li, C.; Wu, X.; Chen, H.; et al. Development of low-alloyed and rare-earth-free magnesium alloys having ultra-high strength. *Acta Mater.* **2018**, *149*, 350–363. [CrossRef]
29. Sasaki, T.T.; Yamamoto, K.; Honma, T.; Kamado, S.; Hono, K. A high-strength Mg-Sn-Zn-Al alloy extruded at low temperature. *Scr. Mater.* **2008**, *59*, 1111–1114. [CrossRef]
30. Xu, S.W.; Oh-ishi, K.; Kamado, S.; Uchida, F.; Homma, T.; Hono, K. High-strength extruded Mg-Al-Ca-Mn alloy. *Scr. Mater.* **2011**, *65*, 269–272. [CrossRef]
31. Garces, G.; Pérez, P.; Barea, R.; Medina, J.; Stark, A.; Schell, N.; Adeva, P. Increase in the Mechanical Strength of Mg-8Gd-3Y-1Zn Alloy Containing Long-Period Stacking Ordered Phases Using Equal Channel Angular Pressing Processing. *Metals* **2019**, *9*, 221. [CrossRef]
32. Wang, Y.; Chen, M.; Zhou, F.; Ma, E. High tensile ductility in a nanostructured metal. *Nature* **2002**, *419*, 912–915. [CrossRef] [PubMed]
33. Wang, Y.M.; Ma, E. Three strategies to achieve uniform tensile deformation in a nanostructured metal. *Acta Mater.* **2004**, *52*, 1699–1709. [CrossRef]

34. Witkin, D.; Lee, Z.; Rodriguez, R.; Nutt, S.; Lavernia, E. Al-Mg alloy engineered with bimodal grain size for high strength and increased ductility. *Scr. Mater.* **2003**, *49*, 297–302. [CrossRef]
35. Wang, H.Y.; Yu, Z.P.; Zhang, L.; Liu, C.G.; Zha, M.; Wang, C.; Jiang, Q.C. Achieving high strength and high ductility in magnesium alloy using hard-plate rolling (HPR) process. *Sci. Rep.* **2015**, *5*, 17100. [CrossRef] [PubMed]
36. Yamasaki, M.; Hashimoto, K.; Hagihara, K.; Kawamura, Y. Effect of multimodal microstructure evolution on mechanical properties of Mg-Zn-Y extruded alloy. *Acta Mater.* **2011**, *59*, 3646–3658. [CrossRef]